Resonant magnetic scattering of polarized soft x rays: Specular reflectivity and Bragg diffraction from multilayers

Maurizio Sacchi
Laboratoire pour l'Utilisation du Rayonnement Electromagnétique, Centre Universitaire Paris-Sud, 91405 Orsay, France and Istituto Nazionale di Fisica della Materia, Sezione di Modena, Via Campi 213/a, 41100 Modena, Italy

Coryn F. Hague
Laboratoire de Chimie Physique–Matière et Rayonnement, Université Pierre et Marie Curie, 11 rue Pierre et Marie Curie, 75231 Paris Cedex 05, France and Laboratoire pour l'Utilisation du Rayonnement Electromagnétique, Centre Universitaire Paris-Sud, 91405 Orsay, France

Eric M. Gullikson and James H. Underwood
Center for X-ray Optics, Materials Sciences Division, Ernest Orlando Lawrence Berkeley National Laboratory, University of California, Berkeley, California 94720

(Received 11 June 1997)

We have measured resonant magnetic scattering of elliptically polarized soft x rays from magnetically ordered Fe/Co multilayers, tuning the photon energy across the $2p$ edges of Fe and Co. Specular reflectivity was measured for a series of angles of incidence as a function of the photon energy. Bragg diffraction was measured performing $\theta/2\theta$ scans for several photon energies. In both cases, large magnetic signals were observed, up to 20% peak to peak in the asymmetry ratio. An estimate of the variation of the real part of the refractive index through the Fe L_3 edge is derived from the Bragg peak displacement versus energy. [S0163-1829(98)00401-9]

I. INTRODUCTION

Magnetic effects on elastic x-ray scattering (Bragg diffraction, specular reflectivity or diffuse scattering) are a well-known phenomenon.[1–3] They represent a powerful tool for investigating magnetic materials since, as has been shown,[4–6] they are strongly enhanced when the photon energy is tuned across an absorption edge (resonant process). The resonant enhancement of the magnetic scattering has mainly been investigated at high photon energies[7–10] in order to match the Bragg law for the typical lattice spacings of crystals. In the soft x-ray range, even larger effects are expected, working, for instance, at the $2p$ edges of transition metals of the first row or at the $3d$ edges of rare earths (300–1500 eV), but the corresponding long wavelengths prevent the use of single crystals. Two approaches have been adopted recently in this energy range: (1) The study of the Bragg diffraction from artificial structures of appropriate $2d$ spacing.[11,12] (2) The analysis of the specular reflectivity, which contains analogous information but has no constraints related to the lattice spacing.[13–17] Both approaches have their own specific advantages: for instance, working under Bragg conditions provides information about the (magnetic) periodicity in ordered structures, while resonant reflectivity can easily be related to electronic properties and absorption spectra. An important aspect common to all the *resonant* x-ray-scattering techniques is the element selectivity which is inherent to working at a specific absorption edge: under these conditions, x-ray scattering in fact becomes a spectroscopy.

II. EXPERIMENT

The aim of our experiment was to compare the magnetic signal in reflectivity and diffraction from a given (multilayer) sample, but at the same time we also wanted to test the feasibility of resonant magnetic scattering experiments using elliptically polarized soft x rays from a bending magnet beamline. The measurements were performed on the Advanced Light Source beamline 6.3.2 at Berkeley.[18] The beamline, based on a Hettrick-Underwood design, has no entrance slits to the monochromator, which uses a varied line-space grating, and features several mechanical solutions which guarantee high stability and ease of operation. In order to change the polarization state of the light without affecting either the optical alignment of the beamline or the calibration of the energy scale, we simply modified the position of the vertical jaws that define the angular acceptance at the entrance of the monochromator. Linearly polarized light is obtained when selecting a vertical accepted angle symmetric with respect to the orbit plane of the electrons in the ring. To have elliptically polarized light of positive (negative) helicity, only the portion of the beam emitted above (below) the orbit plane should go through the monochromator. A good compromise between flux and polarization rate was found accepting the beam within the (0.17 ± 0.05) mrad angular range above the orbit plane. In these conditions, the circular polarization rate of the collected photons (not affected by the grazing incidence monochromator) is calculated to be about 60% in the energy range that we used (650–850 eV). The exit slits were set at 50 μm, for a resolving power of 1200 and a flux of $\approx 10^{10}$ photons s^{-1} on the sample at the Fe $2p$ edges.

Measurements were performed on *ex situ* deposited metallic layers, as well as on multilayers and crystals. The samples were magnetized along the intersection between the surface and scattering planes by a permanent magnet placed

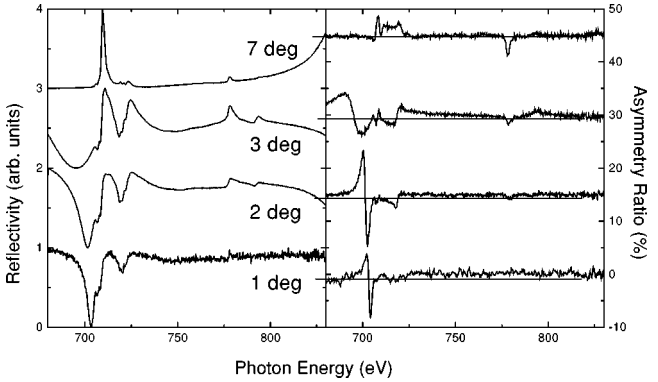

FIG. 1. Reflectivity curves (left panel) taken at different angles of incidence as a function of the photon energy, over a range including the $2p$ absorption edges of both Fe and Co. The sample is a 11.5 Å Fe / 20 Å Co, Fe-terminated multilayer. The right panel shows the corresponding asymmetry, i.e., the ratio between the difference and the sum of the reflectivity curves measured for opposite helicity/magnetization orientations.

behind the sample holder generating a field of approximately 800 G at the sample position. The magnet could be rotated in vacuum around the axis normal to the sample surface, using a stepper motor.[19] In this way we could change the relative orientation between photon helicity and sample magnetization for each scan without affecting the sample alignment. In the end station of line 6.3.2 the scattering plane is vertical (i.e., orthogonal to the plane of the ring). The sample and the detector can be rotated around the same axis in an independent or coupled $\theta/2\theta$ mode. We performed energy scans at fixed scattering angles and also $\theta/2\theta$ scans at fixed photon energies. θ is measured relative to the sample surface.

III. RESULTS

Figure 1 reports the magnetization-averaged reflectivity curves for an Fe/Co multilayer (11.5 Å Fe / 20 Å Co, Fe-terminated) measured at different angles of incidence θ over a photon energy range including both Fe and Co $L_{2,3}$ edges. The right panel of Fig. 1 shows the corresponding magnetic part of the resonant scattering, presented as the asymmetry ratio $(I^+-I^-)/(I^++I^-)$, where $I^\pm$ is the intensity for the photon helicity parallel or antiparallel to the magnetization. The strong angular dependence of both reflectivity and

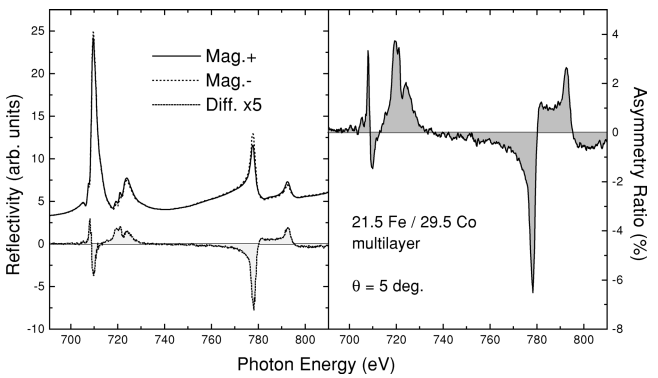

FIG. 2. Resonant reflectivity curves for opposite magnetization directions in a 21.5 Å Fe / 29.5 Å Co multilayer. The difference ($\times 5$) and the asymmetry ratio (right panel) are also given.

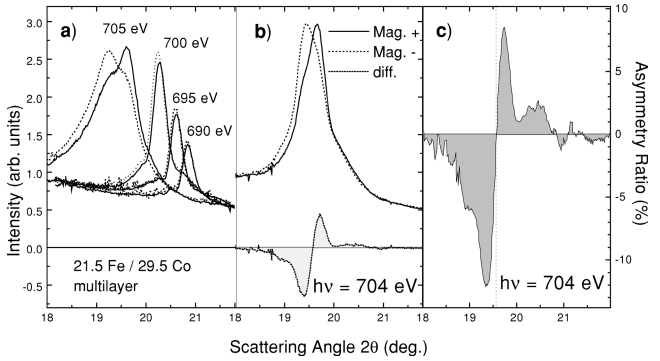

FIG. 3. $\theta/2\theta$ scans at different photon energies close to the Fe L_3 edge (a). Continuous and dotted lines are for opposite magnetization directions. The difference curve (b) for $h\nu=704$ eV and the asymmetry ratio (c) are also given.

asymmetry curves is related to the interference between the real and imaginary parts of the refractive index through Fresnel's equations. It can also be noted in Fig. 1 that for $\theta=1°$ the reflectivity is almost constant away from the Fe $2p$ energy region and the signal from Co (second layer) can hardly be detected. Figure 2 shows in more detail the reflectivity spectrum measured at $\theta=5°$ for a different Fe/Co multilayer (21.5 Å Fe / 29.5 Å Co): the curves for opposite magnetizations and their difference are reported in the left panel, while on the right we have the asymmetry ratio. The fine structure that can be clearly observed in between the L_3 and L_2 iron edges indicates that, when working on metals, a resolving power of $\approx 1\times 10^3$ is sufficient for a detailed analysis of both the reflectivity and its magnetization dependence.

On the same sample, we also measured the Bragg diffraction from the periodic structure of the multilayer, when the photon energy approaches the $2p$ resonances. Figure 3(a) shows a few examples of a series of $\theta/2\theta$ scans taken for

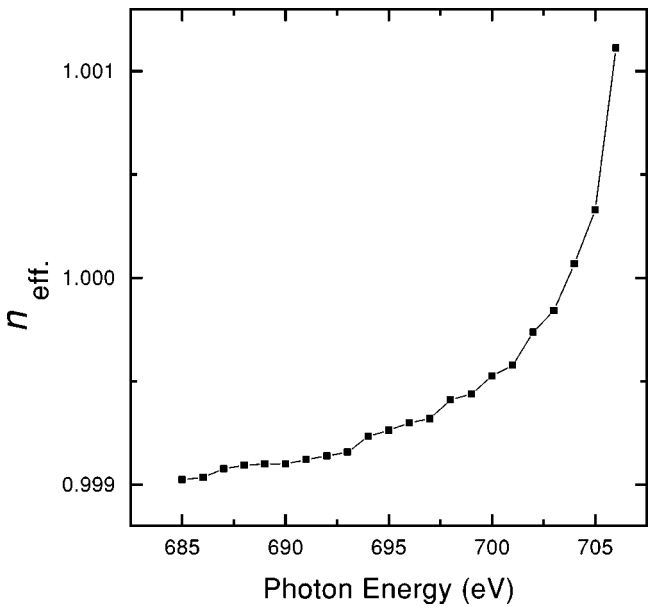

FIG. 4. Photon energy dependence of the effective refractive index n_{eff} value for the 21.5 Å Fe / 29.5 Å Co multilayer, as obtained from the Bragg peak position.

various photon energies just below the Fe $2p_{3/2}$ edge. For each energy, two curves are reported corresponding to opposite magnetization/helicity orientations. Apart from an increased intensity of the diffraction peak, there is also an evident enhancement of the variation with the magnetic field when the photon energy gets closer to the edge. The result of a $\theta/2\theta$ scan taken at 704 eV is shown together with the corresponding asymmetry ratio [Figs. 3(b) and 3(c), respectively]. The displacement with the photon energy of the Bragg peak on the angle scale is certainly related to the change in wavelength, but it persists even when the curves are plotted versus the scattering vector $4\pi\sin\theta/\lambda$. This energy dependence originates from the sharp variations in the real part of the refractive index n close to an absorption edge. The effective n value for the multilayer as a function of the photon energy is plotted in Fig. 4. These values were obtained from the Bragg peak position θ_B according to the approximate relation

$$n_{eff} \approx \left(\frac{\lambda}{2d \sin\theta_B} \right) \sin^2\theta_B + \cos^2\theta_B = \frac{\lambda}{2d} \sin\theta_B + \cos^2\theta_B .$$

For the multilayer spacing d we took the nominal value of 51 Å. The curve in Fig. 4 should still vary for higher photon energies, and larger magnetic effects are expected at the exact $2p_{3/2}$ edge position (about 707 eV for Fe), but we could not see a diffraction peak there. The reason is that for our sample a photon incident at about 9° has to travel through approximately 275 Å of Fe to be reflected at the first Fe/Co interface and come out again. This distance is larger than the absorption length at the maximum of the Fe L_3 edge, hence photons of 707–710 eV can hardly feel the periodic structure of the multilayer. In general, the Bragg peak is bound to get broader at resonance since the increased absorption reduces the number of planes scattering in phase. If the Bragg peak remains measurable (low oscillator strength and/or reduced thickness of the absorbing element for a given $2d$ of the multilayer), data can easily be corrected for absorption and still give very useful information.[11,12]

The enhanced surface sensitivity in the proximity of a resonance is also indicated by the appearance in Fig. 3(a) of a second Bragg peak. Combined absorption measurements in total electron yield mode (probing depth ≈ 20–30 Å) indicate that a partial oxidation of the top layer might be at the origin of the altered Bragg peak position through a change of the actual top layer thickness and/or of its refractive index.

IV. CONCLUSIONS

We have performed resonant magnetic scattering experiments on Fe/Co multilayers, measuring both specular reflectivity and Bragg diffraction at the $2p$ resonances. Specular reflectivity has the advantage of being free from constraints on the existence of a periodic structure and on the value of its lattice parameter. The preliminary measurements that we performed to characterize our experimental setup were conducted on a simple Fe film deposited on silicon and in a previous work a Ni single crystal was studied: in both cases, no Bragg peak would have been available at the $2p$ resonances. Figure 1 also shows that the probing depth of resonant reflectivity can be roughly tuned to enhance near surface contributions. Finally, working at grazing angles gives high reflectance and, consequently, fast data collection (about 20 min to measure one atomic layer of nickel on copper[20]). On the other hand, resonant Bragg diffraction is a unique tool to investigate the periodicity and interface roughness of multilayers, both in terms of structure and magnetism. Moreover, Fig. 4 shows another interesting application of this technique, namely it provides access to a direct determination of the real part of the index of refraction through an absorption resonance.

In conclusion, both specular reflectivity and Bragg diffraction represent important tools for characterizing magnetic materials, especially in the form of thin films and multilayers. Given their absolute compatibility in terms of experimental setup, they should be performed together whenever possible. The maximum magnetic asymmetry ratio obtainable depends on the adopted geometry, but it is easily as high as observed in absorption or even higher.[13–17] Together with its intrinsic photon-in–photon-out character, this makes the technique perfectly suited for semiquantitative magnetometry (element specific hysteresis loops, orientation of easy axes, etc.). In this experiment, we have also shown that the monochromator and the end station of beamline 6.3.2 at the Advanced Light Source are perfectly suited for resonant magnetic scattering experiments in the soft x-ray range. The location of the beamline on a bending magnet source means that a wide energy range may be covered with only smooth variations of the incoming intensity, albeit at the price of a lower flux. Together with easy tunability of the polarization state, this represents a major advantage over an insertion device delivering high flux in narrow energy bands, for this kind of spectroscopy.

ACKNOWLEDGMENT

The authors would like to thank the staff of the Advanced Light Source for efficient help.

[1] O. Klein and Y. Nishina, Z. Phys. **52**, 853 (1929).
[2] P. M. Platzman and N. Tzoar, Phys. Rev. B **2**, 3556 (1970).
[3] F. de Bergevin and M. Brunel, Phys. Lett. **39A**, 141 (1972).
[4] D. Gibbs, D. R. Harshman, E. D. Isaacs, D. B. McWhan, D. Mills, and C. Vettier, Phys. Rev. Lett. **61**, 1241 (1988).
[5] J. P. Hannon, G. T. Trammell, M. Blume, and D. Gibbs, Phys. Rev. Lett. **61**, 1245 (1988).
[6] E. D. Isaacs, D. B. McWhan, C. Peters, G. E. Ice, D. P. Siddons, J. B. Hastings, C. Vettier, and O. Vogt, Phys. Rev. Lett. **62**, 1671 (1989).
[7] P. Carra, M. Altarelli, and F. de Bergevin, Phys. Rev. B **40**, 7324 (1989).
[8] D. Gibbs, G. Grübel, D. R. Harshman, E. D. Isaacs, D. B.

McWhan, D. Mills, and C. Vettier, Phys. Rev. B **43**, 5663 (1991).
[9] C. C. Tang, W. G. Stirling, G. H. Lander, D. Gibbs, W. Herzog, P. Carra, B. T. Thole, K. Mattenberger, and O. Vogt, Phys. Rev. B **46**, 5287 (1992).
[10] F. de Bergevin, M. Brunel, R. M. Galéra, C. Vettier, E. Elkaïm, M. Bessière, and S. Lefèbvre, Phys. Rev. B **46**, 10772 (1992).
[11] J. M. Tonnerre, L. Sève, D. Raoux, G. Soullié, B. Rodmacq, and P. Wolfers, Phys. Rev. Lett. **75**, 740 (1995).
[12] C. F. Hague, J.-J. Gallet, J.-M. Mariot, and M. Sacchi, in *Raman Emission by X-rays*, edited by D. Ederer and J. H. McGuire (World Scientific, Singapore, 1996), p. 137.
[13] C. C. Kao, J. B. Hastings, E. D. Johnson, D. P. Siddons, G. C. Smith, and G. A. Prinz, Phys. Rev. Lett. **65**, 373 (1990).
[14] C. C. Kao, C. T. Chen, E. D. Johnson, J. B. Hastings, H. J. Lin, G. H. Ho, G. Meijs, J.-M. Brot, S. L. Hubert, Y. U. Idzerda, and C. Vettier, Phys. Rev. B **50**, 9599 (1994).
[15] M. Sacchi, J. Vogel, and S. Iacobucci, J. Magn. Magn. Mater. **147**, L11 (1995).
[16] V. Chakarian, Y. U. Idzerda, C.-C. Kao, and C. T. Chen, J. Magn. Magn. Mater. **165**, 52 (1997).
[17] M. Sacchi, Surf. Rev. Lett. **4**, 343 (1997).
[18] J. H. Underwood *et al.*, Rev. Sci. Instrum. (to be published).
[19] C. F. Hague, J.-M. Mariot, and J.-J. Gallet, Appl. Phys. A (to be published).
[20] M. Sacchi, S. Iacobucci, and J. Rife (unpublished).